Similar metabolic responses of co-occurring post-settlement mussels to temperature change despite distinct geographical distributions

Nel, Adel; Quaid, Christopher D. ; Duna, Olwethu O. ; Gimenez Noya, Luis; Porri, Francesca

Marine Biology

DOI:
10.1007/s00227-022-04147-3

Published: 01/01/2023

Peer reviewed version

Similar metabolic responses of co-occurring post-settlement mussels to temperature change despite distinct geographical distributions

Aldi Nel[1,2*], Christopher D. McQuaid[2], Olwethu O. Duna[1,2], Luis Giménez[3,4], Francesca Porri[1,2]

[1] South African Institute for Aquatic Biodiversity, Private Bag 1015, 6140 Grahamstown, South Africa

[2] Department of Zoology and Entomology, Rhodes University, 6140 Grahamstown, South Africa

[3]Alfred Wegener Institute, Helmholtz Centre for Polar and Marine Research, Biologische Anstalt Helgoland, Helgoland, Germany

[4] School of Ocean Sciences, Bangor University, Anglesey, United Kingdom

*Corresponding author: aldipieterse1@gmail.com

ABSTRACT:

For marine animals with biphasic life stages, different environmental conditions are experienced during ontogeny so that physiological constraints on early stages could explain adult distributions and life history traits. The invasive and cool-temperate adapted *Mytilus galloprovincialis* intertidal mussel approaches the eastern limit of its biogeographic distribution on the south coast of South Africa, where it shares a habitat with the warm-temperate adapted and indigenous *Perna perna* mussel. As adults, the two species exhibit different metabolic regulation capacities in response to temperature. We compared the acute metabolic response to temperature between species during the post-settlement recruit stage. Aerobic respiration rates of recently settled recruits were measured monthly for five months for temperatures 5 °C above or below the ambient field seawater temperature at the time of collection. Unlike adults, the capacity for aerobic metabolic regulation in response to temperature differed little between species under the conditions tested, indicating a similar degree of phenotypic or developmental plasticity in response to the thermal environment. In addition, monthly variations in metabolic patterns indicate unexpectedly high plasticity in response to recent seasonal thermal history for both species.

KEY WORDS: Phenotypic plasticity, Ontogeny, Thermal acclimation, Bivalve, Intertidal, Marginal habitats, Mytilidae, Respirometry

INTRODUCTION

Since species fitness, their life history characteristics and ultimately their biogeographic distribution are driven by environmental tolerance and metabolic capacity (Brown 1984; Brown et al. 2004; Verberk et al. 2016), establishing metabolic sensitivity to abiotic factors is important for understanding the dynamics among co-occurring species. Living within an optimal temperature range is particularly important for ectotherms since temperature directly affects metabolism and other physiological functions and rates (Pörtner 2002; Angiletta et al. 2010).

Population distribution is influenced by animal fitness through different life stages (Byrne and Przeslawski 2013), especially for species with biphasic life cycles. Both acclimation potential and environmental tolerance limits can vary with ontogeny and age in marine ectotherms (Byrne 2011; Freda et al. 2019). For example, post-settlement juvenile mussels, referred to as "recruits", often have a higher capacity for rapid phenotypically plastic responses to temperature (Lou et al. 1982; Gleason et al. 2018) as compared to adults. This could be explained by developmental plasticity and adjustment to a new environment (Peyer et al. 2010). Through developmental plasticity, the thermal regime experienced during early life stages influences fitness and thermal tolerance ranges in advanced stages (Stillwell et al. 2005; Cavieres et al. 2019). Adult mussels display thermal tolerances based on local adaptation (Zardi et al. 2011; Tagliarolo and McQuaid 2015), however, understanding the limits of distribution requires establishing the thermal sensitivities and phenotypic plasticity for their earlier ontogenetic stages (Gleason et al. 2018; Truebano et al. 2018).

Interspecific differences in thermal sensitivity influence the fitness of competing co-occurring species. In South Africa, the invasive *Mytilus galloprovincialis* dominates mussel populations on the cool-temperate west coast (Zardi et al. 2007a; McQuaid et al. 2015) and shows partial habitat segregation with the indigenous *Perna perna* on the warm-temperate

58 south coast, where *M. galloprovincialis* dominates the upper mussel zone and *P. perna* the
59 lower shore, with overlap in the middle (Bownes and McQuaid 2006, 2009). This simple
60 pattern emerges from complex effects concerning dispersal, recruitment and adult
61 interactions (McQuaid et al. 2015), including differences in physiological responses to
62 temperature change and thermal stress in adults (Tagliarolo and McQuaid 2015). Adult *M.*
63 *galloprovincialis* display a lower heating activation energy in metabolism (heart rate)
64 compared to the eastern lineage of *P. perna*, indicating a lack of acclimation, and a lower
65 cooling activation energy compared to the co-occurring western *P. perna* lineage, indicating
66 metabolic efficiency at cool temperatures (Tagliarolo and McQuaid 2015). There is currently
67 no information available on the physiological competitive strategies of the early stages of
68 post-settlement co-occuring *P. perna* and *M. galloprovincialis* recruits where both primarily
69 settle in the low-intertidal zone (Porri et al. 2007; Bownes and McQuaid 2009) and display
70 similar survival there as opposed to the high intertidal zone (Bownes and McQuaid 2009).
71 We hence expected post-settlement *M. galloprovincialis* to be more sensitive to fluctuation to
72 high temperature due to its cool-temperate biogeographical adaptation and to therefore
73 display a lower degree of plasticity or an alternative regulating response, as seen during
74 emersion in adults (Tagliarolo and McQuaid 2015). Here, we used respirometry to compare
75 the acute metabolic response to temperature change and metabolic plasticity of co-occurring
76 recruits of *P. perna* and *M. galloprovincialis* as a possible contributor to the biogeographic
77 limit of *M. galloprovincialis* distribution on the south coast.

78 **MATERIALS AND METHODS**

79 **Collection of mussel recruits**

80 Newly recruited *Perna perna* and *Mytilus galloprovincialis* were collected monthly between
81 May 2018 (year henceforth denoted as '18') and February 2019 (henceforth '19'), in Algoa
82 Bay, South Africa (33°98' S, 25°67' E), using 8–10 filamentous plastic scouring pads

(Menge 1992; Bownes et al. 2008; Figure 1) at fixed positions 50–100 cm apart. These were fastened to a flat rock (3 x 4 m) within the low intertidal zone. Small recruits (<765 µm and <686 µm for *Mytilus* and *Perna*; Bownes et al. 2008) were collected for all sampling months, except for Oct 18 and Jan 19, when the average size comprised 'large recruits' (> 765 µm; Bownes et al. 2008).

A sealed Thermochron iButton temperature logger was attached adjacent to one scouring pad to record temperature every thirty minutes for the month preceding the collection of pads. Intertidal site air temperatures for sampled months were: 14.1–21.1 °C (May 18, minimum–maximum), 9.6–21.1 °C (Jul 18), 10.6–22.6 °C (Aug 18), 12.6–32.6 °C (Oct 18), 15.6–31.1 °C (Dec 18) and 13.6–32.6 °C (Jan 19). Estimated periods of immersion and associated temperatures (Table 1) were identified as those occurring between sharp spikes in temperature increase or decrease (Monaco et al. 2019). The scouring pads were transported in a plastic container filled with a thin layer of seawater to maintain humidity, and kept moderately cool with a single ice brick during the 90 minutes of transportation from the field site to the laboratory. The seawater temperature at the time and point of collection was recorded through three consecutive instantaneous measurements using a thermocouple to set the ('at collection') temperature employed at the controlled-temperature laboratory at the Aquatic Ecophysiology Research Platform (AERP) of the South African Institute for Aquatic Biodiversity (Grahamstown, South Africa).

In the temperature-controlled room, scouring pads were submerged in unfiltered seawater collected at the sampling site in two 10 L plastic containers and aerated using air pumps. Depending on the number of scouring pads in the containers, the whole volume of seawater was exchanged for fresh seawater kept at the same temperature once or twice a day. One to three scouring pads were processed per day to collect individual recruits, which were

then placed in 0.5 μm filtered seawater at collection temperature for trials on the following day. This allowed for a fasting period of 18–24 hours prior to respirometry measurements.

Respirometry

Daytime oxygen consumption was measured during immersion to record aerobic metabolism during valve opening (McMahon 1988; Tagliarolo and McQuaid 2015), using a closed respirometry system. Prior to the experiments, recruits were maintained in aerated freshly filtered seawater in a water bath set at collection temperature.

The oxygen consumption of different sets of animals was measured at the field seawater 'collection' temperature and two others respectively at 5 °C above or below this (hereafter '+5 °C' and '-5 °C' treatment, respectively). The '+5 °C' and '-5 °C' temperature change covered what we anticipated to be the thermal ranges experienced by the recruits during immersion, while aiming to stimulate a metabolic response (Paschke et al. 2018). Measurements were conducted for a maximum of seven days following collection from the field. To measure oxygen consumption at the +5 °C and -5 °C temperatures, recruits were gradually exposed to the new temperature, at a ramping rate of 0.17 °C per minute for 30 minutes (Tagliarolo and McQuaid 2015). This ramping was followed by a 90-minute acclimation period at the +5 °C and -5 °C temperatures before transfer to respirometry chambers.

The recruits were viewed under a stereo microscope to select healthy-looking individuals, which responded to gentle stimuli through valve closure, and transferred into 21 individual respirometry chamber wells (80 or 200 μL) in a Loligo® Systems (Denmark) 24-well multiplate with optical fluorescence-based oxygen sensors (SensorDish® Reader SDR2, PreSens, Germany). Three remaining wells, which contained no recruits, were used as controls for background bacterial respiration rates and were subtracted from experimental

recruit respiration rates. Freshly filtered seawater maintained at the measurement temperature was used to fill up the wells to a convex meniscus, and the microplate was sealed by a sheet of parafilm, then a silicon seal, finally followed by a compression block. The sealed multiplate was transferred to a temperature sensor equipped experimental water chamber (Figure 1) which recirculated externally through a programmed water bath. The multiplate was kept under darkness for measurements of standard oxygen consumption rates (Nelson and Chabot 2011; Vorsatz et al. 2021). Oxygen concentration in the wells was recorded for 60–90 minutes at three-minute intervals until a linear decrease in oxygen levels reached 60 % of the initial levels in the wells to maintain a linear relationship between oxygen level and time (Jupe et al. 2020).

Following respirometry, the recruits were placed in 100 % ethanol and subsequently measured using an Olympus SZX16 stereo microscope with a built-in camera and Stream Essentials image capturing and analysis software. Shell length (the longest distance from the umbo to the furthest posterior tip), shell height (the longest distance between the dorsal and ventral shell margins) and width (the longest width of the dorsal view) were measured (Bownes et al. 2008). The volume (L) of each animal was assumed to be that of an ellipsoid (Filgueira et al. 2006) and calculated as: (π/6) x shell height (dm, decimeter) x length (dm) x shell width (dm). Respiration rates (MO_2) in nanomoles O_2 min^{-1} were calculated from the linear slope of the change in O_2 over time, during the incubation period, multiplied by the remaining chamber volume (L) (chamber volume minus the volume of the animal). Total dry mass (µg) values were determined from dry mass (µg) vs. length (mm) regression relationships calculated for bivalve veliger larvae by James (1987) as follows: dry mass (µg) = 47.386 x (shell length in mm)$^{3.663}$. Recruit sizes varied within and between months and was an essential covariate. Using length and allometrically calculated dry masses produced the same model output.

156 **Statistical analysis**

157 Preliminary analyses comparing size-corrected metabolic rates (see below) between replicate
158 days within the same month, using Kruskal-Wallis and Wilcoxon ranks sum tests, confirmed
159 that replicates could be pooled ($p > 0.05$).

160 To establish the most important determinants of MO_2, best-fit mixed generalised least
161 squares (GLS) regression models were fitted using maximum likelihood estimates (R© 4.0.2
162 statistical software; R Development Core Team 2020) and the 'nlme' package (Pinheiro et al.
163 2012). This analysis is robust to variance differences among the different months that
164 comprised the present study. Linear regressions of MO_2 (nmol O_2 min^{-1}) vs dry mass (µg)
165 were fitted after log_{10}-log_{10} transformations using GraphPad Prism 9.0 (GraphPad Software,
166 San Diego California, USA). All MO_2 and dry mass data were logarithm transformed prior to
167 analyses due to the linear relationships between log_{10}-log_{10} MO_2 and dry mass (Chang &
168 Hou 2005). Mass-specific metabolic rates (nmol O_2 min^{-1} μg^{-1}) were calculated for
169 visualisation. Due to variability in size ranges among months, the MO_2 response variable was
170 adjusted for the size covariate by fitting a GLS model with the covariate, and by generating a
171 new corrected $MO2_c$ response variable from the residuals (step 2). This was done separately
172 for each species, prior to selection of model variables (Zuur et al. 2009). Separately for the -5
173 °C and the +5 °C treatment, the selection of significant model variables among species,
174 temperature ('collection' vs. +5 °C or 'collection' vs. -5 °C), month and the interactions
175 among them, was conducted based on the best-fit Akaike's information criterion (AIC) for
176 variables that best explained MO_2 (Table S1). The AIC was used for backward model
177 selection (Zuur et al. 2009). Significant p-values (ANOVA) for interactions further informed
178 model selection when AIC values were similar. Post-hoc Tukey HSD test-95 % family-wise
179 confidence levels for interaction ANOVA models corresponding to the full GLS model

(Table S1) informed on pairwise differences between temperature treatments and species within each month.

The two species did not always settle in each month, and it was therefore not possible to do a full factorial model comparing species responses to both +5 °C and -5 °C temperatures for all months. The effects of species and temperature (+5 °C or -5 °C) were thus evaluated in six separate comparisons. The first two comparisons tested for the combined effects of species and temperature, separately for the +5 °C and -5 °C temperatures ('Species and +5 °C' and 'Species and -5 °C' models). Subsequently, four tests determined responses to temperature treatment for each species (size-corrected MO_2 in response to +5 °C or -5 °C and month): '*Mytilus* and -5 °C', '*Mytilus* and +5 °C', '*Perna* and -5 °C' and '*Perna* and +5 °C'.

Arrhenius plots, describing the relationship between the natural logarithm of mass-specific respiration rate (ln R) and temperature (T), were calculated as $\ln R = \ln a - E/k * 1/T$ (Arrhenius 1889). The slope ($-E/k$) defines the Arrhenius activation energy (E) and was compared between species and among months using GraphPad Prism 9.0. The slopes and intercepts ($\beta 0$ and $\beta 1$) of all linear regression lines were compared using a t-test, where the difference between two regression coefficients is divided by the difference of their respective standard errors (Zar 1984).

RESULTS

Respirometry measurements were performed for months during which enough recruits had settled (Table 1). Lower numbers of animals were tested at the highest temperature

200 (collection + 5 °C) of 26 °C as linear relationships between oxygen decline and time was
201 difficult to obtain due to lower oxygen tension.

202 **Effects of species and temperature on MO_2**

203 *Perna* and *Mytilus* recruits reacted similarly to both -5 °C and +5 °C temperatures (Table S1)
204 as species was not a significant variable for metabolic rate. For both the 'Species and -5 °C'
205 and 'Species and +5 °C' comparisons, temperature was a significant determinant of metabolic
206 rate ($p < 0.001$). There were interactions between species and temperature as species differed
207 within Dec 18 for the -5 °C and +5 °C temperatures (Figure 2 and 3), when *Perna* recruits
208 displayed lower metabolic rates for the -5 °C temperature and higher rates for the +5 °C
209 temperature. There was an interaction between species and month in Oct 18 where species
210 differed for the collection temperature within Oct 18 (Figure 2 and 3), probably owing to
211 relatively larger sizes of *Perna* recruits collected in that month (Table S2). The best-fit
212 (selected) models displayed similar fits (AIC) compared to the full models which
213 incorporated three-way interactions between species, month and temperature (Table S1).
214 Within May 18 and Dec 18, *Mytilus* metabolic rates were significantly higher for the +5 °C
215 compared to the collection temperature which was not the case for *Perna* (Figure 3).
216 Additionally, there were no differences between species for Arrhenius slopes for either the -5
217 °C (Oct 18 and Dec 18; $F = 0.5$ and 2.3, $p = 0.5$ and 0.1 respectively) or the +5 °C
218 temperatures (May 18, Jul 18, Oct 18 and Dec 18; $F = 0.3–1.2$, $p = 0.3–0.6$).

219 The effects of temperature and temperature-month interactions on *Mytilus* metabolic
220 rates were significant for both the -5 and +5 °C temperatures (ANOVA, $p < 0.001$). *Mytilus*
221 metabolic rates at -5 °C temperatures were lower than at collection temperatures within May
222 18 and Jul 18 (Figure 4A), whereas metabolic rates at +5 °C were higher than those at
223 collection temperatures within May 18 and Dec 18 (Figure 3 and 4B). Arrhenius slopes for

224 *Mytilus* differed only among months for the +5 °C temperatures where metabolic activation
225 energies were higher in May 18 than all other months except Dec 18 (Table 2).
226 For *Perna*, temperature and month interactions on metabolic rate were significant for the +5
227 °C temperature ($p < 0.001$). Lower metabolism at the -5 °C temperature than at the collection
228 temperature was observed within Jan 19 (Figure 4C), while higher metabolic rates at the +5
229 °C temperature than the collection temperature were recorded within May 18 and Jan 19
230 (Figure 4D). The Arrhenius slopes were higher in Jan 19 than all other months (Table 2) for
231 both -5 and +5 °C temperatures.

232 **DISCUSSION**

233 The aerobic metabolic response of mussel recruits to temperature change was similar between
234 species and varied across months for both species. We expected inter-specific differences in
235 physiological response to increased temperature due to *M. galloprovincialis*' dominance in
236 the cool-temperate west coast and the study site's proximity to the warm edge of *M.*
237 *galloprovincialis*' distribution on the southeast coast. Here, the transition between the cooler
238 warm-temperate biogeographic region and the warmer subtropical region limits the northern
239 spread of *M. galloprovincialis* (Harrison 2002; Assis et al. 2015). Instead, we found similar
240 activation energies and therefore physiological sensitivities for warming for both species.
241 Despite their recent spread along the southeast coast and low genetic heterogeneity among
242 populations (Zardi et al. 2007a), acclimation to warmer waters at the biogeographic edge
243 could modulate metabolic response. Towards the warm edge of their distribution range in
244 Chile, *Scurria zebrina* limpets displayed higher thermal optima temperatures compared to
245 populations in the centre of their biogeographic range (Broitman et al. 2018). Similar to
246 observations in the present study, adult *M. galloprovincialis* individuals sampled at St Francis
247 Bay (approximately 80 km west of Algoa Bay), South Africa, displayed similar metabolic
248 activation energies in response to warming compared to co-occurring *P. perna* (Tagliarolo

249 and McQuaid 2015). Acclimation and the development of tolerance to a warmer and more
250 variable environment may occur during early ontogeny through differential expression of
251 various physiological and morphological traits (Peyer et al. 2010; Ravaux et al. 2016; Lardies
252 et al. 2021), shaping thermal tolerance limits in adults (Ravaux et al. 2016).
253 Higher metabolism in response to increased temperature in the present study occurred
254 within warmer months (Dec 18 and Jan 19 for *M. galloprovincialis* and *P. perna*,
255 respectively), when the +5 °C was 1–2 °C higher than the maximum submerged temperature,
256 and for May 18, when the +5 °C was 3 °C higher than the maximum temperature
257 experienced. Both early post-settlement *Mytilus* and *Perna* could therefore increase their
258 metabolism effectively at warmer temperatures, suggesting metabolic plasticity for both
259 species during the post-settlement phase. In contrast to the similar inter-specific cooling
260 activation energies for recruits in the present study, adult *M. galloprovincialis* individuals
261 displayed lower activation energies in response to cooling compared to co-occurring *P. perna*
262 in St Francis Bay (Tagliarolo and McQuaid 2015), in agreement with biogeographic
263 distribution. Both *Perna perna* and *Mytilus galloprovincialis* recruits were similarly
264 insensitive to decreased temperature in early summer (Dec 18), again suggesting similar
265 metabolic plasticity for both species. Unfortunately, no species comparisons were made for
266 decreased temperature response within cooler months or within Jan 19, due to uneven
267 numbers for species as *Perna* display seasonal dependance of reproductive output whereas
268 *Mytilus* does not (Zardi et al. 2007b). Low metabolic rates at cool temperatures for *Perna*
269 recruits during the warmest month of Jan 19 reflected a lack of cool temperature acclimation.
270 In contrast, cool temperature-adapted mussels can maintain normal standard metabolic rates
271 and low activation energies during temperature decreases, as did *M. galloprovincialis* adults
272 (Tagliarolo & McQuaid 2015). For *Mytilus*, there was an interaction between decreased
273 temperature and month for metabolic rates, and lower metabolic rate in response to decreased

temperature occurred within the months that comprised lower temperature ranges (May 16 and Jul 18), indicating seasonal patterns.

A transplant experiment for *Mytilus californianus* has shown that juvenile mussels (shell length 5–14.5 mm) can adjust their thermal tolerance range within one month where adults cannot (Gleason et al. 2018). Similarly, developmental plasticity likely contributed to seasonal patterns of thermal acclimation observed in the present study. A high degree of phenotypic plasticity during development can be adaptive when plastic phenotypes directly result from spatial environmental heterogeneity like temporary pools for tadpoles (Lind and Johansson 2007; Beldade et al. 2011) or the intertidal environment. The degree of developmental phenotypic plasticity varies with egg size and species in echinoid *Strongylocentrotus* larvae as *S. franciscanus* display higher plasticity in feeding organ morphology compared to congeneric *S. purpuratus* larvae (McAlister 2007). In molluscs, a higher degree of developmental plasticity in the freshwater quagga mussel *(Dreissena bugensis*), compared to the congeneric *D. polymorpha*, facilitates its wider habitat use in the Great Lakes of North America (Peyer et al. 2010).

In the present study, it is interesting that both *Mytilus* and *Perna* recruits displayed a similar degree of metabolic plasticity in response to temperature, as shown by their inter-specific Arrhenius activation energies, despite their different biogeographical distributions. Future studies should combine comparisons of the metabolic response to warming temperature between the two species with oxidative stress markers to understand how these species regulate metabolic efficiency (Salin et al. 2015).

At recruitment stage, *Mytilus* and *Perna* within the same lower intertidal environment can display similar thermal sensitivities in aerobic metabolism, the basis for aerobic scope, regardless of seasonal variation in expected thermal exposure, and despite different biogeographic distribution ranges. To fully understand inter-species competition on the south

coast for early life stages, future studies should establish the thermal performance curves for both species for controlled acclimation regimes simulating both summer and winter, using narrow size ranges. Additionally, sensitivities to other environmental factors, such as the interaction between temperature and aerial exposure, should be established.

CONCLUSION

Early post-settlement *Mytilus* and *Perna* mussels were both able to increase aerobic respiration when exposed to increased temperature during warmer months, despite *Mytilus* being close to the warm limit of its distribution range. Both species adjusted their thermal responses to the temperature range they were recently exposed to during the preceding month, displaying similar activation energies and plasticity. Metabolic plasticity in post-settlement mussels are most likely driven by developmental plasticity, although complex metabolic interactions between factors such as cohort, size, and population may also be at play.

Conflict of Interest

We have no conflicts of interest to disclose.

Compliance with ethical standards

All applicable international, national, and/or institutional guidelines for the care and use of animals were followed. Collection permit from the department of environmental affairs of the Republic of South Africa: RES2019/30.

Acknowledgements

This research was funded by the South African Research Chairs Initiative of the Department of Science and Technology and the National Research Foundation to CDM (Grant number 64801). Aldi Nel was supported by a grant holder-linked postdoctoral bursary from the National Research Foundation (NRF) and the South African Institute for Aquatic

323 Biodiversity (SAIAB) African Coelacanth Ecosystem Programme (ACEP). Use of
324 infrastructure and equipment was provided by the SAIAB-NRF Aquatic Ecophysiology
325 Research Platform (AERP) at Rhodes University.

326 *Data Availability*

327 Data will be made available on reasonable request.

328 *Authors' Contribution*

329 Data collection and establishment of experimental protocols were performed by A Nel and O
330 Duna, while study conceptualization and manuscript writing was performed by A Nel, CD
331 McQuaid, L Giménez and F Porri. The experimental equipment, methods and resources were
332 governed by CD McQuaid and F Porri.

333 **REFERENCES**

334 Arrhenius S (1889) Über die Dissociationswärme und den Einfluss der Temperatur auf
335 den Dissociationsgrad der Elektrolyte. Z Phys Chem 4:226–248

336 Assis J, Zupan M, Nicastro KR, Zardi GI, McQuaid CD, Serrão EA (2015)
337 Oceanographic conditions limit the spread of a marine invader along Southern African
338 shores. PLoS ONE 10(6):e0128124

339 Beldade P, Mateus AR, Keller RA (2011) Evolution and molecular mechanisms of
340 adaptive developmental plasticity. Mol Ecol 20:1347–1363.

341 Bownes SJ, McQuaid CD (2006) Will the invasive mussel *Mytilus galloprovincialis*
342 Lamarck replace the indigenous *Perna perna* L. on the south coast of South Africa? J Exp
343 Mar Biol Ecol 338:140–151

344 Bownes S, Barker NP, McQuaid CD (2008) Morphological identification of primary
345 settlers and post-larvae of three mussel species from the coast of South Africa. Afr J Mar Sci
346 30:233–240

347 Bownes SJ, McQuaid CD (2009) Mechanisms of habitat segregation between an
348 invasive and an indigenous mussel: settlement, post-settlement mortality and recruitment.
349 Mar Biol 156:991–1006

350 Broitman B, Aguilera MA, Lagos NA, Lardies MA (2018) Phenotypic plasticity at the
351 edge: contrasting population-level responses at the overlap of the leading and rear edges of
352 the geographical distribution of two *Scurria* limpets. J Biogeogr 45:2314–2325

353 Brown JH (1984) On the relationship between abundance and distribution of species.
354 Am Nat 124:255–279

355 Brown JH, Gillooly JF, Allen AP, Savage VM, West GB (2004) Toward a metabolic
356 theory of ecology. Ecology 85:1771–1789

Byrne M (2011) Impact of ocean warming and ocean acidification on marine invertebrate life history stages: vulnerabilities and potential for persistence in a changing ocean. Oceanogr Mar Biol Annu Rev 49:1–42

Byrne M, Przeslawski R (2013) Multistressor studies of the impacts of warming and acidification of the ocean on marine invertebrates' life histories. Integr Comp Biol 53:582–596

Cavieres G, Alruiz JM, Medina NR, Bogdanovich JM, Bozinovic F (2019) Transgenerational and within generation plasticity shape thermal performance curves. Ecol Evol 9:2072–2082

Chang Y, Hou PL (2005) Thermal acclimation of oxygen consumption rate may be seasonally dependent in the subtropical Anuran Latouche's frog (*Rana latouchii*, Boulenger). Physiol Biochem Zool 78:947–955

Filgueira R, Labarta U, Fernández-Reiríz MJ (2006) Flow-through chamber method for clearance rate measurements in bivalves: design and validation of individual chambers and mesocosm. Limnol Oceanogr-Meth 4:284-292

Freda PJ, Ali ZM, Heter N, Ragland GL, Morgan TJ (2019) Stage-specific genotype-by-environment interactions for cold and heat hardiness in *Drosophila melanogaster*. Heredity 123:479–491

Gleason LU, Strand EL, Hizon BJ, Dowd WW (2018) Plasticity of thermal tolerance and its relationship with growth rate in juvenile mussels (*Mytilus californianus*). Proc R Soc B 285:20172617

Harrison TD (2002) Preliminary assessment of the biogeography of fishes in South African estuaries. Mar Freshwater Res 53:479–490.

James AG (1987) Feeding ecology, diet and field-based studies on feeding selectivity of the Cape anchovy *Engraulis capensis* Gilchrist. S Afr J Mar Sci 5:673–692

382 Jupe LL, Bilton DT, Knights, AM (2020) Do differences in developmental mode shape
383 the potential for local adaptation? Ecology 101:e02942
384 Lardies MA, Caballero P, Duarte C and Poupin MJ (2021) Geographical variation in
385 phenotypic plasticity of intertidal sister limpet's species under ocean acidification scenarios.
386 Front. Mar. Sci. 8:647087.
387 Lind MI, Johansson F (2007) The degree of adaptive phenotypic plasticity is correlated
388 with the spatial environmental heterogeneity experienced by island populations of *Rana*
389 *temporaria*. ESEB 20:1288–1297
390 Lou ZK, Liu XS, Chen ZH, Zhang XF, Zhang NS (1982) Experiment on rearing
391 mussels spats in late autumn by raising water temperature. Shuichan Xuebao 6:43–49
392 Menge BA (1992) Community regulation: under what conditions are bottom-up factors
393 important on rocky shores? Ecology 73:755–765
394 McAlister JS (2007) Egg size and the evolution of phenotypic plasticity in larvae of the
395 echinoid genus *Strongylocentrotus*. J Exp Mar Biol Ecol 352:306–316
396 McMahon RF (1988) Respiratory response of periodic emergence in intertidal
397 molluscs. Integr Comp Biol 28:97–144
398 McQuaid CD, Porri F, Nicastro KR, Zardi GI (2015) Simple, scale-dependent patterns
399 emerge from very complex effects: an example from the intertidal mussels *Mytilus*
400 *galloprovincialis* and *Perna perna*. In: Hughes RN, Hughes DJ, Smith IP, Dale AC (eds)
401 Oceanography and Marine Biology: An Annual Review. CRC Press, Boca Raton, p 127–156
402 Monaco CJ, Porporato EMD, Lathlean JA, Tagliarolo M, Sarà G, McQuaid CD (2019)
403 Predicting the performance of cosmopolitan species: dynamic energy budget model skill
404 drops across large spatial scales. Mar Biol 166:14

405 Nelson JA, Chabot D (2011) General energy metabolism. In: Farrell AP (ed)
406 Encyclopedia of fish physiology: from genome to environment. Academic Press, California,
407 p 1566–1572
408 Paschke K, Agüero J, Gebauer P, Díaz F, Mascaró M, López-Ripoll E, Re D, Caamal-
409 Monsreal C, Tremblay N, Pörtner H-O and Rosas C (2018) Comparison of aerobic scope for
410 metabolic activity in aquatic ectotherms with temperature related metabolic stimulation: A
411 novel approach for aerobic power budget. Front Physiol 9:1438
412 Peyer SM, Hermanson JC, Lee CE (2010) Developmental plasticity of shell
413 morphology of quagga mussels from shallow and deep-water habitats of the Great Lakes. J
414 Exp Biol 213:2602–2609
415 Pinheiro J, Bates D, DebRoy S, Sarkar D (2012) nlme: linear and nonlinear mixed
416 effects models. R package version 3
417 Porri F, Zardi GI, McQuaid CD, Radloff S (2007) Tidal height, rather than habitat
418 selection for conspecifics, controls settlement in mussels. Mar Biol 152:631–637
419 Pörtner HO (2002) Climate variations and the physiological basis of temperature
420 dependent biogeography: systemic to molecular hierarchy of thermal tolerance in animals.
421 Comp Biochem Physiol A 132:739–761
422 Ravaux J, Léger N, Rabet N, Fourgous C, Voland G, Zbinden M, Shillito B (2016)
423 Plasticity and acquisition of the thermal tolerance (upper thermal limit and heat shock
424 response) in the intertidal species *Palaemon elegans*. J Exp Mar Biol Ecol 484:39–45
425 R Development Core Team (2020) R: a language and environment for statistical
426 computing. R Foundation for Statistical Computing, Vienna
427 Salin K, Auer SK, Rey B, Selman C, Metcalfe NB (2015) Variation in the link between
428 oxygen consumption and ATP production, and its relevance for animal performance. Proc R
429 Soc B 282:20151028

Stillwell RC, Fox CW (2005) Complex patterns of phenotypic plasticity: interactive effects of temperature during rearing and oviposition. Ecology 86:924–934

Tagliarolo M, McQuaid CD (2015) Sub-lethal and sub-specific temperature effects are better predictors of mussel distribution than thermal tolerance. Mar Ecol Prog Ser 535:145–159

Truebano M, Fenner P, Tills O, Rundle SD, Rezende EL (2018) Thermal strategies vary with life history stage. J Exp Biol 22:jeb171629

Verberk WCEP, Bartolini F, Marshall D, Pörtner HO, Terblanche JS, White CR, Giomi F **(**2016) Can respiratory physiology predict thermal niches? Ann N Y Acad Sci 1365:73–88

Vorsatz LD, Pattrick P, Porri F (2021) Fine-scale conditions across mangrove microhabitats and larval ontogeny contributes to the thermal physiology of early stage brachyurans (Crustacea: Decapoda). Conserv Physiol 9:coab010

Zar JH (1984) Comparing simple linear regression equations. In: Chapter 18, *Biostatistical Analysis*, 2nd edition, Prentice-Hall

Zardi GI, McQuaid CD, Teske PR and Barker NP (2007a) Unexpected genetic structure of mussel populations in South Africa: indigenous *Perna perna* and invasive *Mytilus galloprovincialis*. Mar Ecol Prog Ser 337:135–144

Zardi GI, McQuaid CD, Nicastro KR (2007b) Balancing survival and reproduction: seasonality of wave action, attachment strength and reproductive output in indigenous *Perna perna* and invasive *Mytilus galloprovincialis* mussels. Mar Ecol Prog Ser 334:155–163

Zardi GI, Nicastro KR, McQuaid CD, Hancke L, Helmuth B (2011) The combination of selection and dispersal helps explain genetic structure in intertidal mussels. Oecologia 165:947−958

Zuur AF, Ieno EN, Walker NJ, Saveliev AA, Smith, G. (2009) Mixed Effects Models and Extensions in Ecology with R. Springer, New York

455

456 Table 1: The monthly mean (T_{Mean}) and minimum to maximum (T_{Min}–T_{Max}) seawater
457 temperatures are displayed for thirty-minute interval temperature recordings prior to animal
458 sampling (N = 904–1187). The coefficient of variation (% C.V.) for monthly submerged
459 temperatures was low at 3.0–8.7 %. The T_{Mean} and T_{Min}–T_{Max} for water temperatures during
460 the previous seven days ($_7$) are displayed in parentheses. The temperatures (T_{Exp}) used for
461 recruit respirometry for each sampling are displayed as temperature at the time of
462 'collection', and +5 and -5 °C, respectively.

Month	**T_{Mean}**	**T_{Min}–T_{Max}**	**(T_{Mean}, T_{Min}–T_{Max})$_7$**	**T_{Exp}**
May 18	18.0 °C	16.1–20.1 °C	(17.8, 16.1–18.6 °°C)	18, 23 and 13 °C
Jul 18	16.8 °C	15.1–18.6 °C	(16.8, 16.1–17.6 °C)	17, 22 and 12 °C
Aug 18	16.1 °C	14.6–17.6 °C	(16.1, 15.1–17.1 °C)	16 and 21 °C
Oct 18	18.5 °C	14.6–22.6 °C	(19.0, 14.6–22.6 °C)	17, 22 and 12 °C
Dec18	20.9 °C	17.1–24.1 °C	(21.2, 18.1–24.1 °C)	21, 26 and 16 °C
Jan 19	21.8 °C	18.1–24.6 °C	(21.7, 18.1–24.6 °C)	21, 26 and 16 °C

463

Table 2: The slope β1 (± S.E.) and intercept β0 (± S.E.) parameters are displayed for Arrhenius plots between the natural logarithm of mass-specific respiration rate (ln *R*) and inverse temperature (1/T). For each test temperature and species, significant differences in β1and β0 over different months are denoted by different letter superscripts read vertically.

	Mytilus		***Perna***	
	β1	**β0**	**β1**	**β0**
T_{Low}				
May 18	-8.1 (4.3)^{a}	19.3 (15.0)^{a}		
Jul 18	-15.9 (3.6)^{a}	47.6 (12.4)^{b}		
Oct 18	-4.02 (4.4)^{a}	5.5 (15.2)^{a}	4.6 (3.6)^{a}	-25.1 (12.6)^{a}
Dec 18	-5.81 (2.7)^{a}	12.6 (9.2)^{c}	-2.4 (3.9)^{a}	1.0 (13.6)^{b}
Jan 19			-15.1 (3.9)^{b}	43.3 (13.5)
T_{High}				
May 18	-17.9 (3.9)^{a}	53.18 (13.2)	-13.5 (5.5)^{a}	38.2 (18.8)^{a}
Jul 18	-6.8 (3.7)^{b}	16.3 (12.5)^{a}	-3.4 (5.4)^{a}	4.5 (18.6)^{b}
Aug 18	-4.8 (5.3)^{b}	8.3 (18.2)^{b}		
Oct 18	0.4 (4.8)^{b}	-9.6 (16.4)^{b}	-7.4 (5.3)^{a}	16.3 (18.2)^{c}
Dec 18	-12.5 (3.7)^{ab}	35.2 (12.5)^{c}	-20.9 (7.7)^{ab}	63.9 (26.0)^{bd}
Jan 19			-40.0 (5.9)^{b}	127.9 (20.0)^{e}

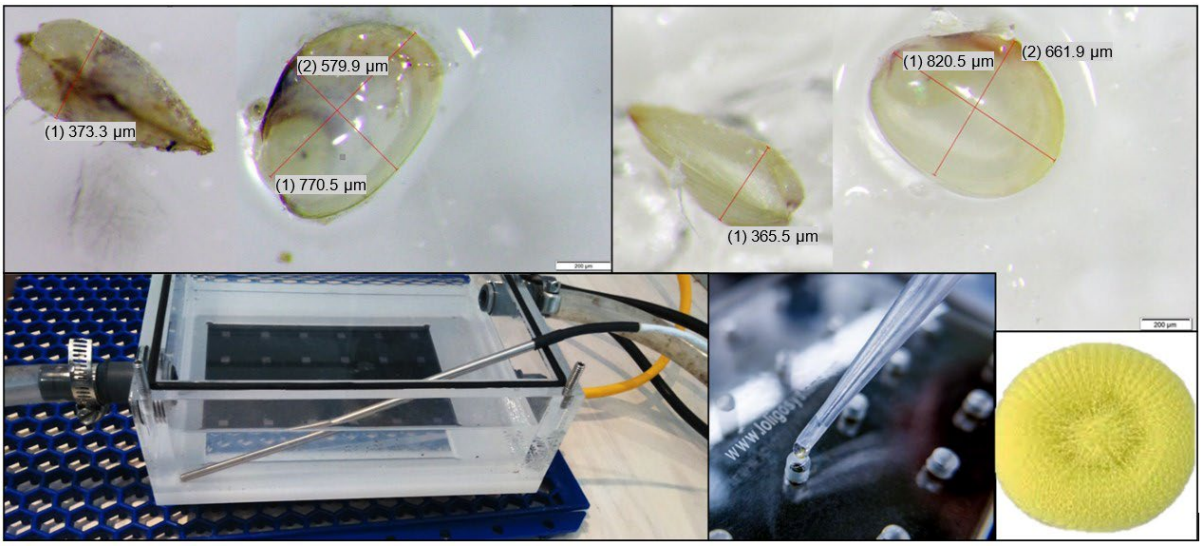

Figure 1: *Mytilus* (top left) and *Perna* (top right) recruits are displayed. Bottom (from left to right); the circulating water bath, respirometry wells (80 µL), and collection scouring pad for mussel recruits.

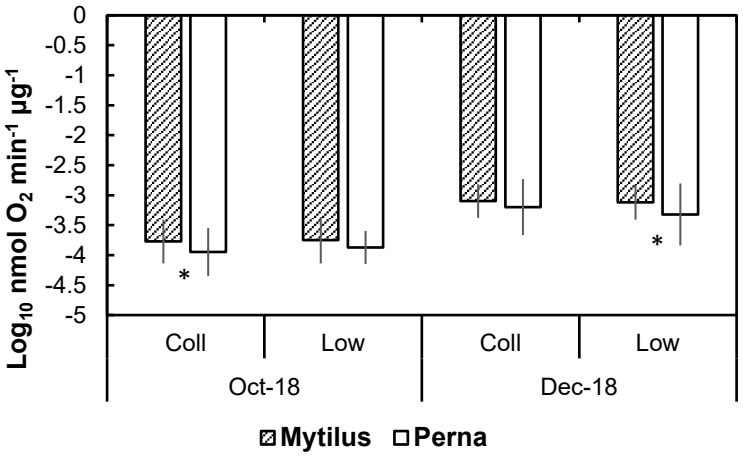

Figure 2: Mean (± S.D.) logarithm transformed mass-specific oxygen consumption values for *Mytilus* (N = 16–53) and *Perna* (N = 23–43) recruits in response to the -5 °C ("Low") and collection ("Coll") temperatures ("Species and -5 °C") are displayed. The "*" denotes differences between species for the collection temperature within Oct 18 and for the low temperature within Dec 18 (Tukey HSD tests for pairwise comparisons for ANOVA testing interactions for -5 °C, month and species).

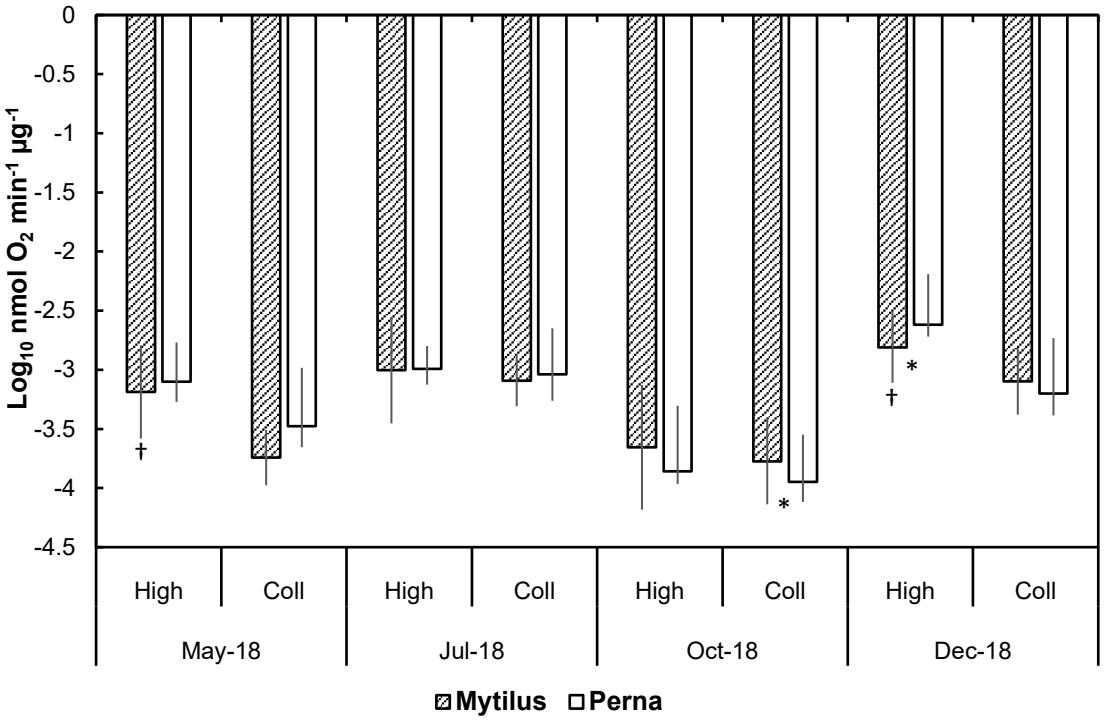

Figure 3: Mean (± S.D.) logarithm transformed mass-specific oxygen consumption values for *Mytilus* (N = 16–53) and *Perna* (N = 6–43) recruits in response to +5 °C ("High") and collection ("Coll") temperatures ("Species and +5 °C") are displayed. The "*" denotes differences between species for the collection treatment within Oct 18 and for the high treatment within Dec 18 (Tukey HSD tests for pairwise comparisons for ANOVA testing interactions for +5 °C, month and species). The "†" denotes differences between high and collection temperatures for *Mytilus* species within May 18 and Dec 18.

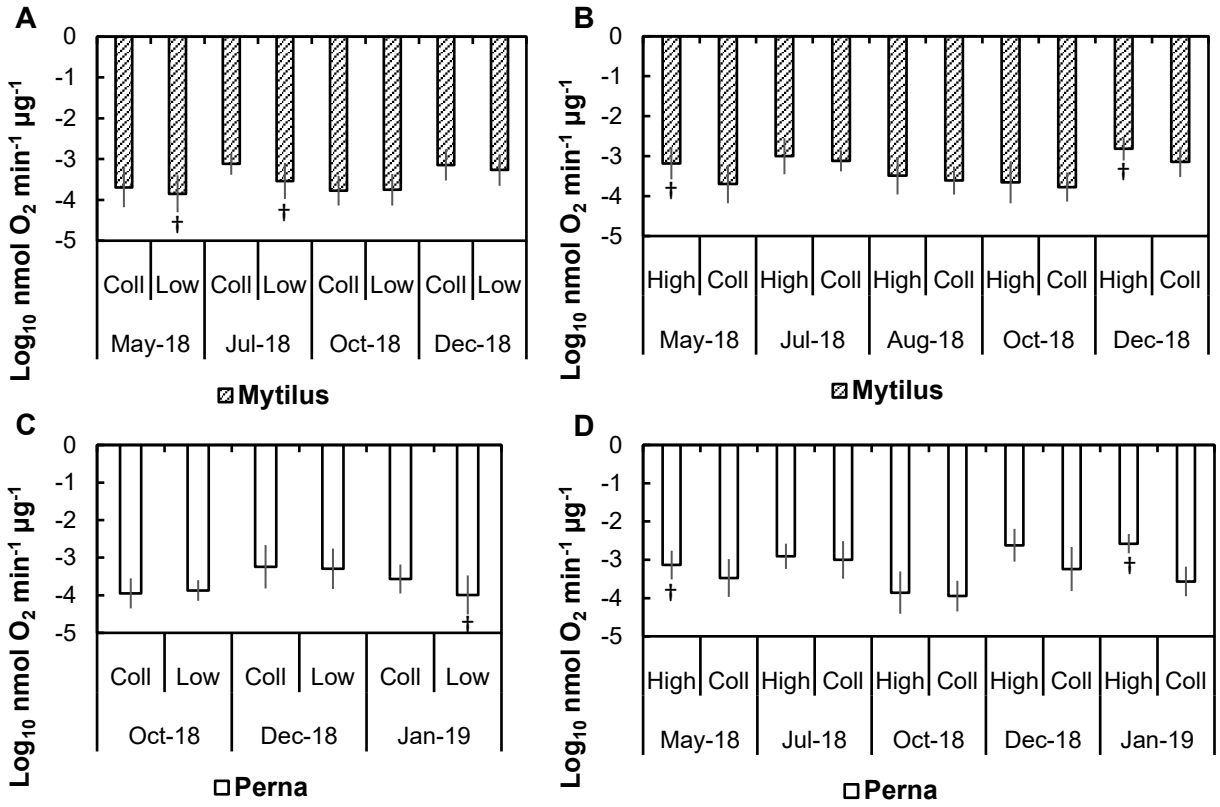

Figure 4: Mean (± S.D.) logarithm transformed mass-specific oxygen consumption values are displayed. Tukey HSD tests for pairwise comparisons of ANOVA interactions for temperature and month revealed differences (denoted by "†") for *Mytilus* recruits between -5 °C ("Low") and collection ("Coll") temperature ("*Mytilus* and -5 °C", N = 14–49) within May 18 and Jul 18 (A). Differences between "Coll" temperatures and the +5 °C ("High") temperature for *Mytilus* recruits ("*Mytilus* and +5 °C", N = 14–49) occurred within May 18 and Dec 18 (B). For *Perna* recruits, differences between "Coll" temperatures and the -5 °C ("Low") temperature ("*Perna* and -5 °C", N = 22–48) occurred within Jan 19 (C), while differences between "Coll" temperatures and the +5 °C ("High") temperature ("*Perna* and +5 °C", N = 6–41) occurred within May 18 and Jan 19 (D).